

## Materials and Methods

*Materials:* Oligonucleotides were synthesized on a 10 $\mu$ mole scale by standard phosphoramidite chemistry using an Äkta DNA synthesizer, and were purified by repeated DMT on/ DMT off reverse phase HPLC, as previously described.<sup>1,2</sup> To prevent loss of 8oxoG during deprotection, oligonucleotides containing 8oxoG were deprotected in 0.1 M  $\beta$ -mercaptoethanol/ conc. NH<sub>4</sub>OH following the protocols of Johnson and coworkers.<sup>3,4</sup> The purities of the oligonucleotides were assessed by analytical HPLC and ion spray mass spectroscopy, and were found to be better than 98% by mass spectroscopy. Purified oligonucleotides were dialyzed using dispo-dialyzers with MWCO 500 da (Spectrum, CA) against at least two changes of buffer containing 10 mM Cacodylic acid/NaCacodylate, and 0.1 mM Na<sub>2</sub> EDTA and sufficient NaCl to yield a final concentration of 100 mM in Na<sup>+</sup> ions. DNA extinction coefficients of the unmodified parent sequences were determined by phosphate assay under denaturing conditions (90°C)<sup>5,6</sup> and were found to be:  $\epsilon_{X(CAG)_6Y}$  (260nm, 90°C) = 368400 M<sup>-1</sup> cm<sup>-1</sup>;  $\epsilon_{Y'X'}$  (260nm, 90°C) = 186200 M<sup>-1</sup> cm<sup>-1</sup>.<sup>7</sup> For 8oxoG (O) or abasic site (F) containing oligonucleotides, extinction coefficients were determined from continuous variation titrations (Job plots)<sup>8</sup> with the complementary parent oligonucleotides, and were found to be  $\epsilon_{X(CAG)_6Y-F}$  (260nm, 90°C) = 368400 M<sup>-1</sup> cm<sup>-1</sup>;  $\epsilon_{Y'X'-F}$  (260nm, 90°C) = 176000 M<sup>-1</sup> cm<sup>-1</sup>;  $\epsilon_{X(CAG)_6Y-O}$  (260nm, 90°C) = 368400 M<sup>-1</sup> cm<sup>-1</sup>;  $\epsilon_{Y'X'-O}$  (260nm, 90°C) = 186200 M<sup>-1</sup> cm<sup>-1</sup>. As expected, for the 40mers, the impact of a single 8oxoG or abasic site lesion in place of guanine is independent of lesion position and too small to result in a measurable change in extinction coefficient compared to the X(CAG)<sub>6</sub>Y parent 40mer.

*DSC studies:* DSC studies were conducted using a NanoDSCII differential scanning calorimeter (Calorimetry Science Corporation, Utah) with a nominal cell volume of 0.3 ml.<sup>9</sup> Oligonucleotides, at a concentration of 50  $\mu$ M in strand, were repeatedly scanned between 0°C and 90/95 °C with a constant heating rate of 1°C /min, while continuously recording the excess power required to maintain sample and reference cells at the same temperature. After conversion of the measured excess power values to heat capacity units and subtractions of buffer/buffer scans, the raw DSC traces were normalized for DNA concentration and analyzed using Origin software (OriginLab Corporation, Massachusetts). The calorimetric enthalpy ( $\Delta H_{cal}$ ) was derived by integration of the excess heat capacity curve, and  $\Delta C_p$  was derived from the difference in the linearly extrapolated pre- and post-transition baselines at T<sub>m</sub>.  $\Delta S$  was derived by  $\Delta H/T_m$ , assuming “pseudomonomolecular” behavior in which propagation dominates initiation.<sup>10</sup> Although our constructs formally are bimolecular complexes, their concentration dependent denaturation deviates from a molecularity of two, as generally is the case for complexes of this size.<sup>11</sup> The theoretical entropy correction for a strictly bimolecular reaction of 21 cal mol<sup>-1</sup> K<sup>-1</sup> at C<sub>t</sub> = 50  $\mu$ M falls within the uncertainties of our entropy values, and is the same for all our constructs. As a result, inclusion of such a molecularity contribution simply scales the magnitudes, while not altering the relative differences in  $\Delta S$  and  $\Delta G$  between our constructs.  $\Delta G$  at the reference temperature was calculated using

standard equations taking into account the nonzero heat capacity changes. The  $T_m$  is defined as the temperature at the mid point of the integrated excess heat capacity curve for a given conformational transition. At this temperature, for a process that exhibits pseudomonomolecular behavior, the sample is 50% denatured.

*Analysis of experimental heat capacity curves:* The experimental excess heat capacity curves of our  $\Omega$ -DNA's were fit to the following model modified from that originally described by Wyman and Gill for n independent, two-state transitions.<sup>12,13</sup>

$$C_p(T) = \sum_{i=1}^n C_p(T)_i + \frac{\tau^2}{R} * \sum_{i=1}^n \frac{\Delta H(T)_i * \exp[-\Delta H(T)_i * (\tau - \tau_{mi}) / R]}{\{1 + \exp[-\Delta H(T)_i * (\tau - \tau_{mi}) / R]\}^2} \quad \text{eq. (1)}$$

Equation 1 is modified from equation (5.36) given in Wyman and Gill to account for the temperature dependence of the enthalpy ( $\Delta H(T)_i$ ) and to take account of the contributions of the differing native and denatured heat capacity of each of the sub-transitions. The impact of strand dissociation is not considered in this model, because concentration dependent denaturation studies show the denaturation process for our  $\Omega$ -DNA's to behave in a pseudo-monomolecular manner. Nevertheless, we note, that strand separation may slightly impact the shape of the melting curves at high temperature.

In equation 1,  $\tau = \frac{1}{T}$  is the inverse temperature at any point along the curve and

$\tau_{mi} = \frac{1}{T_{mi}}$  is the inverse melting temperature of the i th component;  $\Delta H(T)_i$  is the

enthalpy change associated with unfolding of the i th component at temperature T determined from the enthalpy change at  $T_m$  according to the standard relations:

$$\Delta H(T)_i = \Delta H(T_m)_i - \Delta C_{p_i}(T_{mi} - T) \quad \text{eq. (2a)}$$

and

$$\Delta C_{p_i} = C_{p_i}^D - C_{p_i}^N \quad \text{eq. (2b)}$$

where D and N indicate denatured and native respectively.

We assume that each transition's contribution to the overall heat capacity change is proportional to it's contribution to the overall enthalpy change; specifically

$$\Delta C_{p_i} = \frac{\Delta H(T_m)_i}{\sum_{j=1}^n \Delta H(T_m)_j} \Delta C_p(T^*)$$

where  $\Delta C_p(T^*)$  is the heat capacity change for the overall denaturation process at the

$$\text{weighted average transition temperature } T^* = \frac{\sum_{i=1}^n T_{mi} \Delta H_i}{\sum_{i=1}^n \Delta H_i}.$$

The native and denatured state heat capacities of the  $i$  th component are assumed to change linearly with temperature and are described by equation 3:

$$C_p(T)_i^N = m^N T + C_p(0)_i^N \quad \text{eq. (3a)}$$

The heat capacity of the denatured state differs from that of the native state by  $\Delta C_{p_i}$  at  $T^*$ , that is  $C_p(T^*)_i^D = C_p(T^*)_i^N + \Delta C_{p_i}$  so

$$C_p(T)_i^D = m^D (T - T^*) + C_p(T^*)_i^N + \Delta C_{p_i} \quad \text{eq. (3b)}$$

The imposition of linear models for the temperature dependences of the native and denatured heat capacities with the pre- or post-transition baselines of each transition sharing a common slope  $m^N$  or  $m^D$  may appear somewhat arbitrary, however, we note that the overall experimental excess heat capacity curves outside the melting domain are well described by linear changes in native and denatured heat capacities (see figure S1)

From the temperature dependence of the native and denatured state heat capacities the contribution of the  $i$  th component to the heat capacity baseline,  $C_p(T)_i$  is calculated according to the following relation:

$$C_p(T)_i = \alpha(T)_i C_p(T)_i^N + (1 - \alpha(T)_i) C_p(T)_i^D \quad \text{eq. (4)}$$

where  $\alpha(T)_i$  represents the fraction of the  $i$  th component that remains native at temperature  $T$  and is calculated according to equation 5.

$$\alpha(T)_i = \frac{\Delta H(T)_i - \left\langle \frac{\{\Delta H(T)_i * \exp[-\Delta H(T)_i * (\tau - \tau_{mi}) / R]\}}{\{1 + \exp[-\Delta H(T)_i * (\tau - \tau_{mi}) / R]\}} \right\rangle}{\Delta H(T)_i} \quad \text{eq. (5)}$$

Heat capacity curves were fit using the model described above and the Solver function in Microsoft Excel. The 2n+4 adjustable parameters in the fits were  $T_{mi}$ ;  $\Delta H(T_m)_i$ ,  $\Delta C_p(T^*)$ ,  $C_p(0)^N$ ,  $m^D$  and  $m^N$ .

We fit our experimental data to this model for n = 1, n = 2 and n = 3, and find that we can obtain good agreement between the experimental curves and the fitted curves when n = 2 for all  $\Omega$ -DNA constructs. n = 3 does not give a statistically significant improvement in fit of the experimental parameters, whereas n = 1 never results in a reasonable fit to the experimental data.

#### REFERENCES

- (1) Völker, J.; Klump, H. H.; Breslauer, K. J. *Proc Natl Acad Sci U S A* **2001**, *98*, 7694-7699.
- (2) Völker, J.; Makube, N.; Plum, G. E.; Klump, H. H.; Breslauer, K. J. *Proc Natl Acad Sci U S A* **2002**, *99*, 14700-14705.
- (3) Bodepudi, V.; Shibutani, S.; Johnson, F. *Chem Res Toxicol* **1992**, *5*, 608-617.
- (4) Shibutani, S.; Bodepudi, V.; Johnson, F.; Grollman, A. P. *Biochemistry* **1993**, *32*, 4615-4621.
- (5) Snell, F. D.; Snell, C. T. *Colorimetric methods of analysis, including some turbidimetric and nephelometric methods*; R. E. Krieger Pub. Co.: Huntington, N.Y., 1972.
- (6) Plum, G. E. In *Current Protocols in Nucleic Acid Chemistry*; Beaucage, S. L., Bergstrom, D. E., Glick, G. D., Jones, R. A., Eds.; John Wiley & Sons, Inc., 2000, pp 7.3.1-7.3.17.
- (7) Völker, J.; Klump, H. H.; Breslauer, K. J. *J Am Chem Soc* **2007**, *129*, 5272-5280.
- (8) Job, P. *Annali di chimica* **1928**, *9*, 113-134.
- (9) Privalov, G.; Kavina, V.; Freire, E.; Privalov, P. L. *Anal Biochem* **1995**, *232*, 79-85.
- (10) Marky, L. A.; Breslauer, K. J. *Biopolymers* **1987**, *26*, 1601-1620.
- (11) Pilch, D. S.; Plum, G. E.; Breslauer, K. J. *Curr Opin Struct Biol* **1995**, *5*, 334-342.
- (12) Gill, S. J.; Richey, B.; Bishop, G.; Wyman, J. *Biophys Chem* **1985**, *21*, 1-14.
- (13) Wyman, J.; Gill, S. J. *Binding and Linkage. Functional Chemistry of Biological Macromolecules*; University Science Books: Mill Valley, CA, 1990.

**Figure S2:**

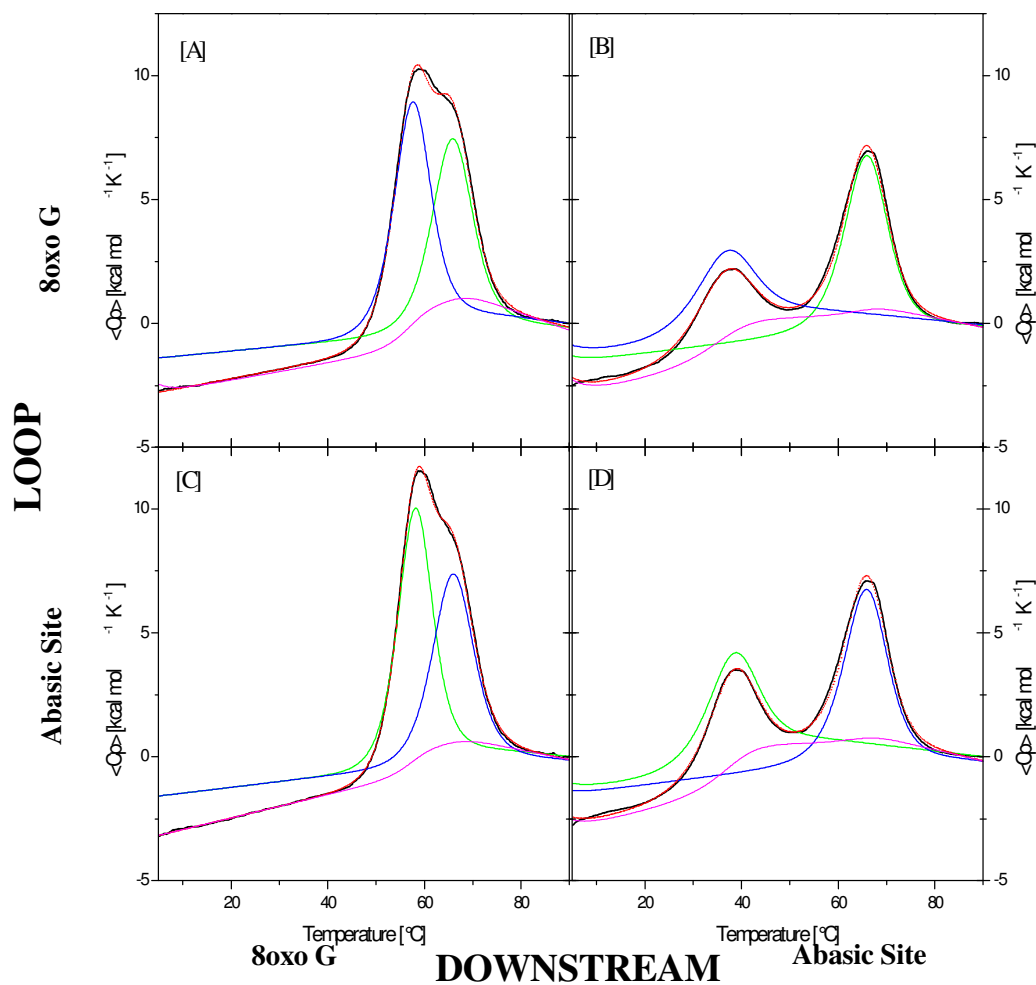


**Figure S2:** Results for the deconvolution of the experimental excess heat capacity curves of the X(3)-X group of dual lesion  $\Omega$ -DNA's. Panel A: O(3)-O; Panel B: O(3)-F; Panel C: F(3)-O; and Panel D: F(3)-F. The experimental excess heat capacity curves are shown in black, while the fitted curves are shown in red. The deconvoluted subtransitions are shown in green (lower temperature peak) and blue (upper temperature peak), and the fitted baseline is shown in magenta. Similar results to those shown here are obtained for all other lesion pairs studied.

**Table S2: Experimentally derived thermodynamic parameters for dual lesion in loop and stem**

Oligomer	T <sub>m</sub> [°C]	ΔH [kcal mol <sup>-1</sup> ]	ΔS [cal mol <sup>-1</sup> K <sup>-1</sup> ]	ΔC <sub>p</sub> [cal mol <sup>-1</sup> K <sup>-1</sup> ]	ΔG [kcal mol <sup>-1</sup> ]
CAG	62.3 ± 0.3	172.7 ± 8.6	515 ± 25	1350 ± 140	16.3 ± 0.8
<b>O(n) · O Family of Lesions</b>					
CAG-O1· CTG-OStem	58.8 ± 0.3	169.0 ± 8.4	509 ± 25	1380 ± 140	14.7 ± 1.1
CAG-O3· CTG-OStem	58.5 ± 0.3	172.3 ± 8.6	520 ± 26	1560 ± 160	14.6 ± 1.1
CAG-O5· CTG-OStem	58.1 ± 0.3	168.8 ± 8.4	510 ± 26	1530 ± 150	14.2 ± 1.0
<b>F(n) · O Family of Lesions</b>					
CAG-F1· CTG-OStem	57.7 ± 0.3	170.4 ± 8.5	515 ± 26	1620 ± 160	14.1 ± 1.0
CAG-F3· CTG-OStem	58.6 ± 0.3	172.5 ± 8.6	520 ± 26	1490 ± 150	14.8 ± 1.1
CAG-F5· CTG-OStem	65.4 ± 0.3	144.3 ± 7.2	426 ± 21	1120 ± 120	14.4 ± 1.1
<b>O(n) · F Family of Lesions</b>					
CAG-O1· CTG-FStem	66.2 ± 0.3 (36.0) (66.2)	134.7 ± 6.7 (42.1) (92.7)	398 ± 20 (136) (273)	N/D	16.3 ± 1.2 <sup>1</sup>
CAG-O3· CTG-Fstem	65.9 ± 0.3 (36.5) (65.9)	131.0 ± 6.6 (46.0) (85.8)	386 ± 19 (149) (253)	N/D	15.8 ± 1.2 <sup>1</sup>
CAG-O5· CTG-FStem	66.1 ± 0.3 (36.4) (66.1)	139.1 ± 6.9 (48.3) (90.8)	410 ± 21 (156) (268)	N/D	16.8 ± 1.3 <sup>1</sup>
<b>F(n) · F Family of lesions</b>					
CAG-F1· CTG-FStem	66.7 ± 0.3 (34.6) (66.7)	127.2 ± 6.4 (36.7) (90.5)	374 ± 19 (119) (266)	N/D	15.6 ± 1.2 <sup>1</sup>
CAG-F3· CTG-FStem	65.8 ± 0.3 (38.4) (65.8)	151.5 ± 7.6 (62.0) (89.9)	447 ± 22 (199) (265)	N/D	18.2 ± 1.4 <sup>1</sup>
CAG-F5· CTG-FStem	65.9 ± 0.3 (36.1) (65.9)	114.6 ± 5.7 (33.2) (81.5)	338 ± 17 (107) (240)	N/D	13.8 ± 1.0 <sup>1</sup>

<sup>1</sup> Not corrected for ΔC<sub>p</sub> effects

**Table S2: Fitted thermodynamic parameters**

Oligomer	$T_m^*$ [°C]	$\Delta H^*_{(fit)}$ [kcal mol <sup>-1</sup> ]	$T_{m1}$ [°C]	$\Delta H_{(1, fit)}$ [kcal mol <sup>-1</sup> ]	$T_{m2}$ [°C]	$\Delta H_{(2, fit)}$ [kcal mol <sup>-1</sup> ]
<b>CAG Ω-DNA</b>	<b>63.0</b>	<b>173.67</b>	<b>60.9</b>	<b>93.95</b>	<b>65.52</b>	<b>79.71</b>
<b>O(n) · O Family of Lesions</b>						
<b>CAG-O1 / O-Downstream</b>	<b>61.1</b>	<b>166.0</b>	<b>57.2</b>	<b>87.56</b>	<b>65.6</b>	<b>78.47</b>
<b>CAG-O3 / O-Downstream</b>	<b>60.8</b>	<b>165.8</b>	<b>57.1</b>	<b>90.2</b>	<b>65.3</b>	<b>75.12</b>
<b>CAG-O5 / O-Downstream</b>	<b>61.1</b>	<b>161.5</b>	<b>56.8</b>	<b>83.49</b>	<b>65.7</b>	<b>78.05</b>
<b>F(n) · O Family of Lesions</b>						
<b>CAG-F1/ O-Downstream</b>	<b>61.0</b>	<b>160.4</b>	<b>56.4</b>	<b>82.91</b>	<b>65.9</b>	<b>77.55</b>
<b>CAG-F3/ O-Downstream</b>	<b>61.5</b>	<b>173.8</b>	<b>58.0</b>	<b>95.43</b>	<b>65.7</b>	<b>78.35</b>
<b>CAG-F5/ O-Downstream</b>	<b>60.07</b>	<b>140.6</b>	<b>54.765.54</b>	<b>64.54</b>	<b>65.7</b>	<b>76.00</b>
<b>O(n) · F Family of Lesions</b>						
<b>CAG-O1/ F-Downstream</b>	<b>49.5</b>	<b>115.3</b>	<b>32.8</b>	<b>56.45</b>	<b>65.6</b>	<b>58.83</b>
<b>CAG-O3/ F-Downstream</b>	<b>50.0</b>	<b>121.25</b>	<b>35.0</b>	<b>61.69</b>	<b>65.4</b>	<b>59.56</b>
<b>CAG-O5/ F-Downstream</b>	<b>49.72</b>	<b>113.8</b>	<b>33.1</b>	<b>55.34</b>	<b>65.4</b>	<b>58.47</b>
<b>F(n) · F Family of lesions</b>						
<b>CAG-F1 / F-Downstream</b>	<b>50.0</b>	<b>110.4</b>	<b>30.3</b>	<b>49.15</b>	<b>65.8</b>	<b>61.27</b>
<b>CAG-F3 / F-Downstream</b>	<b>50.2</b>	<b>130.1</b>	<b>37.2</b>	<b>69.96</b>	<b>65.4</b>	<b>60.09</b>
<b>CAG-F5 / F-Downstream</b>	<b>52.57</b>	<b>100.1</b>	<b>28.6</b>	<b>34.87</b>	<b>65.40</b>	<b>65.22</b>

